IEEE Access
Multidisciplinary | Rapid Review | Open Access Journal

Received June 2, 2020, accepted June 10, 2020, date of publication June 17, 2020, date of current version June 30, 2020.

Digital Object Identifier 10.1109/ACCESS.2020.3002862

A Low-Profile Decoupling Slot-Strip Array for 2 × 2 Microstrip Antenna

DI GAO[1], ZHENXIN CAO[1], (Member, IEEE), XIN QUAN[1], MINQIAN SUN[2], SUIDAO FU[1], AND PENG CHEN[1], (Member, IEEE)

[1]School of Information Science and Engineering, Southeast University, Nanjing 210096, China
[2]State Key Laboratory of Disaster Prevention and Mitigation of Explosion and Impact, Army Engineering University of PLA, Nanjing 210096, China

Corresponding author: Zhenxin Cao (caozx@seu.edu.cn)

This work was supported in part by the National Natural Science Foundation of China under Grant 61471117, in part by the Foundation of Shannxi Key Laboratory of Integrated and Intelligent Navigation (Grant No. SKLIIN-20190204) and the Fundamental Research Funds for the Central Universities (Southeast University, Grant No. 2242020K40114).

ABSTRACT Two-dimensional antennas provide additional variables that can be used to control and shape the pattern, and widely used in engineering applications include tracking radar, communications, direction finding and many others. However, the reduced mutual coupling becomes more complex due to the mode and strength of the mutual coupling field betweensani adjacent elements are different. In this paper, a low-profile decoupling slot-strip array (DSSA) for 2 × 2 microstrip antenna is proposed. The DSSA consists of a slot array etched on the ground plane and a strip array printed on the radiation patches plane. The band-stop effect of the slot array decreases the mutual coupling of both H-plane and D-plane. Meanwhile, the coupling current generated by the induced current on strip array can cancel the coupling current generated by excited current, which can significantly improve the E-plane isolation Additionally, the scattering parameters of other three types of antenna which have the different relative positions of feeding ports are also discussed. To verify the proposed viewpoint, a 2 × 2 antenna with the DSSA is modeled and manufactured. The experimental results demonstrate that a considerable mutual coupling reduction of 33.2 dB for H-plane, 28.5 dB for E-plane, and 24.1 dB for D-plane is achieved while 10 dB bandwidth for S_{11} remains almost unchanged. Fortunately, the experimental results are in good agreement with the simulation results, which confirms that the DSSA has an excellent promising application in two-dimensional antenna.

INDEX TERMS Decoupling slot-strip array, 2 × 2 antenna, mutual coupling reduction, low-profile.

I. INTRODUCTION

Massive multiple-input-multiple-output (MIMO) has been considered as a key technology in wireless communication applications [1], [2]. MIMO technology increases the system capacity by using multiple transmit and receive antenna elements to achieve multipath propagation. However, The mutual coupling among massive elements caused by the spatial radiation or surface wave propagation gives rise to problems such as reduced efficiency, deteriorated radiation pattern, and mismatched input impedance, which degrades the MIMO performance dramatically [3]. Therefore, optimized mutual coupling of MIMO system is in urgent need and would be of significance in wireless communication applications.

Numerous ways have been proposed to decrease the mutual coupling between antennas, such as electromagnetic bandgap (EBG) structure [4]–[6], defected ground structure (DGS) [7]–[11], polarization-conversion isolator [12], resonator [13], neutralization line [14]–[16], coupled resonator decoupling network [17], interference cancellation chip [18] and metamaterial [19]–[21]. However, these decoupling approaches are limited to two-element coupled antennas or one-dimensional antenna array.

For two-dimensional antenna, isolation enhancement is even more knotty. It is not only due to the complex electromagnetic environment caused by the multiple coupling elements and multiple coupling paths but also due to the mode and strength of mutual coupling field between adjacent elements (E-plane, H-plane and D-plane) are different [22].

In the past few years, several studies have been carried out on two-dimensional decoupling antenna [23]–[29]. In [23], an array-antenna decoupling surface (ADS) which is placed in front of the array antenna is first proposed and applied to a 2× 2 antenna. The ADS can cancel the coupled wave by creating another reflective electromagnetic wave.

The measured results show that the mutual coupling between adjacent elements was reduced by more than

The associate editor coordinating the review of this manuscript and approving it for publication was Kai Lu.

15 dB, but the coupling between the diagonal antennas was decreased slightly. The isolation in [24] was enhanced by adjusting the shape of the ground plane (DP) under each element to make the mutual coupling from the free space and the ground plane out of phase. The mutual coupling between both adjacent and diagonal elements is decreased by more than 10 dB. However, both ADS and DP increase the profile of the antenna, which hinder their wider application in low-profile array. The embedded metamaterial EM bandgap decoupling slab introduced in [25] suppresses the surface currents to decrease the mutual coupling between any elements by more than 10 dB. However, the center-to-center spacing of more than 1.5 λ_0 (λ_0 is the vacuum wavelength of the center frequency) makes this method unsuitable for many practical engineering applications.

Based on the above observation, the realization of a low-profile high isolated 2 × 2 microstrip antenna with the center-to-center spacing being 0.5 λ_0 is considered, and a novel decoupling slot-strip array (DSSA) is proposed. The following unique and attractive features will be demonstrated:

1) The DSSA can reduce mutual coupling in four types of 2 × 2 microstrip antenna with different relative positions of feeding ports.
2) The DSSA can decrease the mutual coupling between any two elements (E-plane, H-plane, and D-plane) in 2 × 2 antenna, and achieve about 30 dB isolation enhancement.
3) The DSSA keeps the low-profile and matching condition of the antenna.

This paper is organized as follows. Section II introduces the design of the DSSA, explains the corresponding decoupling mechanisms and demonstrates the effect on mutual coupling reduction. Section III presents the prototype and measured results. The conclusion is drawn in Section IV.

II. DESIGN AND SIMULATION

A. STRUCTURE OF THE LOW-PROFILE HIGH- ISOLATED ANTENNA WITH DSSA

The geometry of the proposed low-profile high isolated 2 × 2 antenna with DSSA is shown in Fig. 1. Each element is fed independently through a SMA connector. The DSSA consists of 12 slots etched on the ground plane and 5 metal strips printed on the radiation patches plane. 8 slots in the slot array are distributed outside the radiating edge of the elements. These 8 slots have the same size and their long sides are perpendicular to the surface current direction. The other 4 slots are 5 mm longer than the 8 slots, and distributed outside the non-radiation edge of the elements. The 5 strips have the same length and the long side is parallel to the current direction of the antenna. The proposed antenna substrate is with parameters as thickness of 3 mm, dielectric constant of 2.55 and loss tangent of 0.006, respectively. The simulated results are carried out using High-Frequency Structure Simulator commercial software.

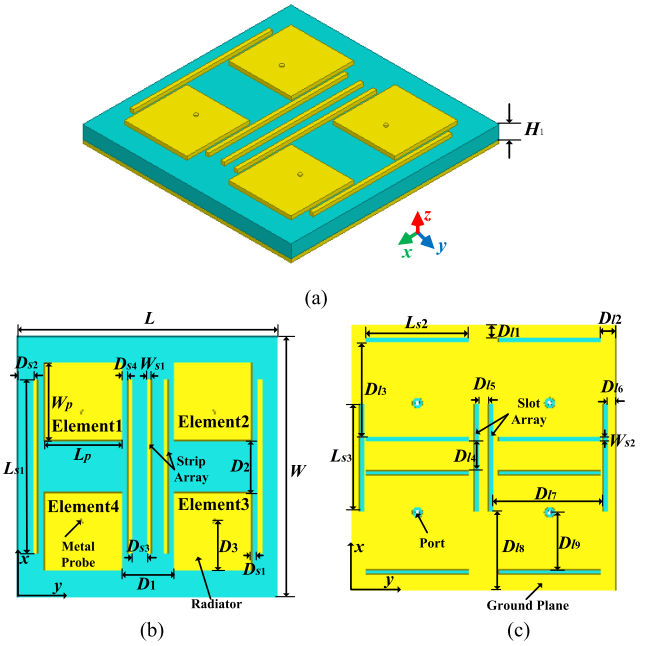

FIGURE 1. Geometry of the 2 × 2 antenna with DSSA. (a) Perspective view. (b) Top view. (c) Lateral view.

TABLE 1. The parameters of the proposed 2 × 2 antenna with DSSA (Unit: mm).

Parameters	Value	Parameters	Value	Parameters	Value
W	240	L	240	Wp	72
Lp	72	$Ls1$	160	$Ls2$	93.2
$Ls3$	97	$Dl1$	14.75	$Dl2$	13.4
$Dl3$	98.75	$Dl4$	29.25	$Dl5$	15.0
$Dl6$	7.5	$Dl7$	103	$Dl8$	111.5
$Dl9$	55	$D1$	48	$D2$	48
$Ds1$	5.5	$Ds2$	14.5	$Ds3$	17
$Ds4$	5.5	$Ws1$	1	$Ws2$	1

Based on the definition in [22], when the elements are positioned collinearly along the E-field direction, this arrangement is referred as E-plane (between element 1 and element 4, between element 2 and element 3). When the elements are positioned collinearly along the H-field direction, this arrangement is referred as H-plane (between element 1 and element 2, between element 3 and element 4). Similarly, when the elements are positioned collinearly along the diagonal direction, this arrangement is referred as D-plane (between element 1 and element 3, between element 2 and element 4). For a two-dimensional antenna, the mutual coupling field are TM modes in a direction of propagation along E-plane and TE modes in a direction of propagation along H-plane. The mode and strength of the mutual coupling field in E-plane and H-plane is different, which makes the

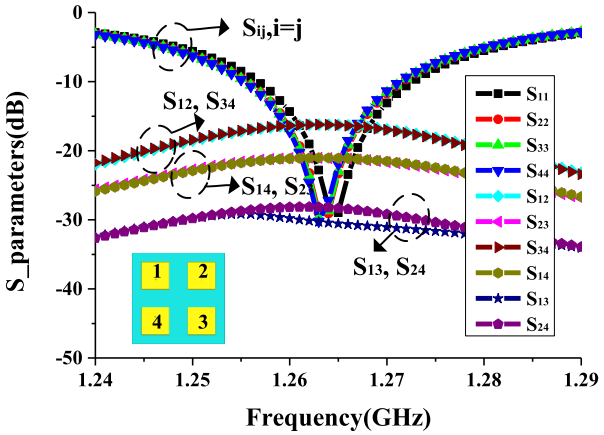

FIGURE 2. S-parameters of the 2 × 2 antenna without DSSA.

decreased mutual coupling in two-dimensional antenna even more knotty.

The simulated S-parameters of the antenna without DSSA are illustrated in Fig. 2. The center frequency is 1.264 GHz with the bandwidth ($S_{ii} < 10$ dB, i = 1∼ 4) of 16 MHz. The mutual coupling between two H-plane coupled adjacent elements S_{12} and S_{34} is 16.2 dB at 1.264 GHz. S_{14} and S_{23} which are the mutual coupling between two E-plane coupled adjacent elements is 21 dB at 1.264 GHz. The isolation of the two D-plane coupled antennas S_{13} and S_{24} are −29.1 dB and 28.2 dB at center frequency, respectively.

B. THE DECOUPLING MECHANISM OF SLOT ARRAY

In the first place, the slot array shown in Fig. 1(c) is etched on the ground plane of the 2 × 2 antenna to reduce the H-plane and D-plane coupling. The vector current distributions of the ground plane with and without the etched slot array in center frequency in Fig. 3 can help to explain the decoupling mechanism.

The operating state of the antenna is that the element 1 is excited and element 2, 3, 4 are terminated with 50 Ω matching load. As shown in Fig. 3, the slot array results in two major effects [30]. The first effect is that the slot array increases the length of the coupling current path, which is equivalent to adding a series inductance L between elements. The second effect is that the potential difference across the slot corresponds to a capacitor C connected in series between the elements. The combined these two effects of the slot array can be modeled by an equivalent LC-parallel lumped element circuit. The qualitative analysis of the LC-parallel circuit shows that the inductance L is obviously positively correlated with the slot length, while the capacitance C is negatively correlated with the slot width. Therefore, by properly optimizing the position and size of the slot array, the circuit can have a band-stop effect to reduce mutual coupling.

Taking the mutual coupling between element 1 and element 2 as an example, the coupling paths between the two elements can be mainly divided in four types as shown in Fig. 4 [31]:

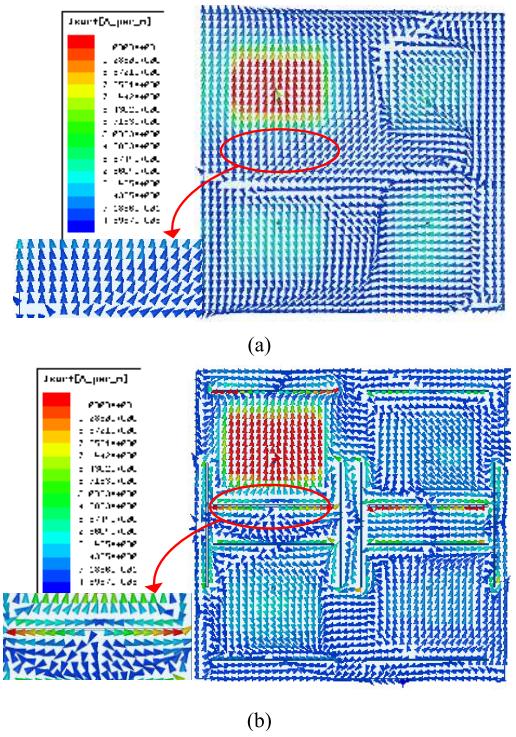

FIGURE 3. The current distribution of the ground plane. (a) Without slot array. (b) With slot array.

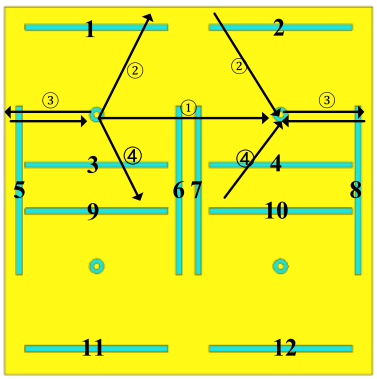

FIGURE 4. The schematic diagram of the main mutual coupling paths between element 1 and 2.

① a coupling wave that is directly propagated from element 1 to element 2; ② a coupling wave that is propagated in the upper area; ③ a coupling wave caused by the reflection from the substrate edges; ④ a coupling wave that is propagated in the lower area. Therefore, a slot array is designed to suppress the mutual coupling due to the multiple coupling paths. The slots with the same size can be equivalent to having the same LC-parallel circuit. The eight slots with the same size as slot 1 are equivalent to L_1 in parallel with C_1, and the four slots with the same size as slot 5 are equivalent to L_2 in parallel with C_2. The slot 6 and slot 7, which are on the same coupling path ①, should be connected in series. The same series circuit applies to slot 1 and slot 2, slot 3 and

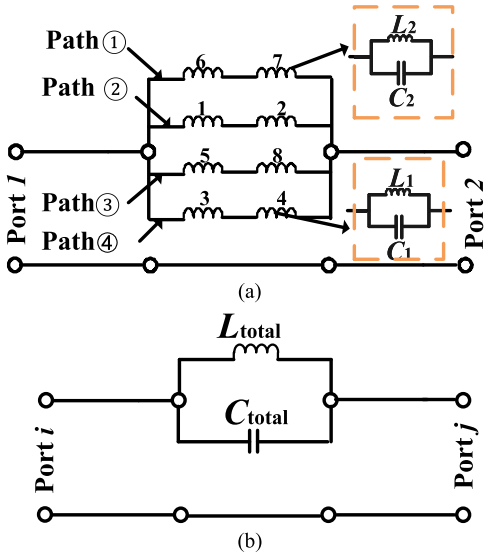

FIGURE 5. Lumped-parameter equivalent circuit model of antenna with the slot array. (a) Between port 1 and Port 2. (b) Between any two elements.

slot 4, slot 5 and slot 8. The four coupling paths should be connected in parallel, as shown in Fig. 5(a). The L total and C total in Fig. 5(b) are the sum effects aroused by the slot array. The above analysis method is also applicable to other two elements. In the equivalent circuit model in Fig. 5(b), the LC-parallel circuit is equivalent to a first-order band-stop filter, which produces a transmission zero in the coupling path between elements. Obviously, the band-stop frequency f_0 depends on the L total and C total and could be deduced from

$$f_0 = \frac{1}{2\pi\sqrt{L_{total}C_{total}}} \tag{1}$$

To verify the proposed equivalent circuit theory, analysis and simulations were performed through the commercial software High-Frequency Structure Simulator (HFSS). Fig. 6 shows the typical mutual coupling S_{12} and S_{13} with different slot length L_{s2}, L_{s3} and slot width W_{s2}. The simulated results show that the decoupling resonant frequency has been shifted to a lower frequency by shorting L_{s2}, L_{s3} and narrowing W_{s2}. The simulated results agree well with the analysis based on the equivalent circuit model.

The simulated S-parameters of the 2 × 2 antenna with slot array are depicted in Fig. 7. The bandwidth of $S_{ii} < -10$ dB is nearly unchanged in contrast to the antenna without slot array. The S_{12} and S_{34} are decreased from –16.2 dB to – 37.4 dB and –39.8 dB, respectively. S_{13} and S_{24} are decreased from –30.4 dB and –28 dB to –37.8 dB at center frequency, respectively. The S_{14} and S_{23} are –23.5 dB, only 2.5 dB lower than the antenna without slot array. This shows that the proposed slot array can effectively reduce both the H-plane and D-plane mutual coupling, and slightly decrease the E-plane mutual coupling. The reason for these results is that the optimized size and position of slot array can only generate transmission zeros on the coupled paths of H- plane and D-plane, rather

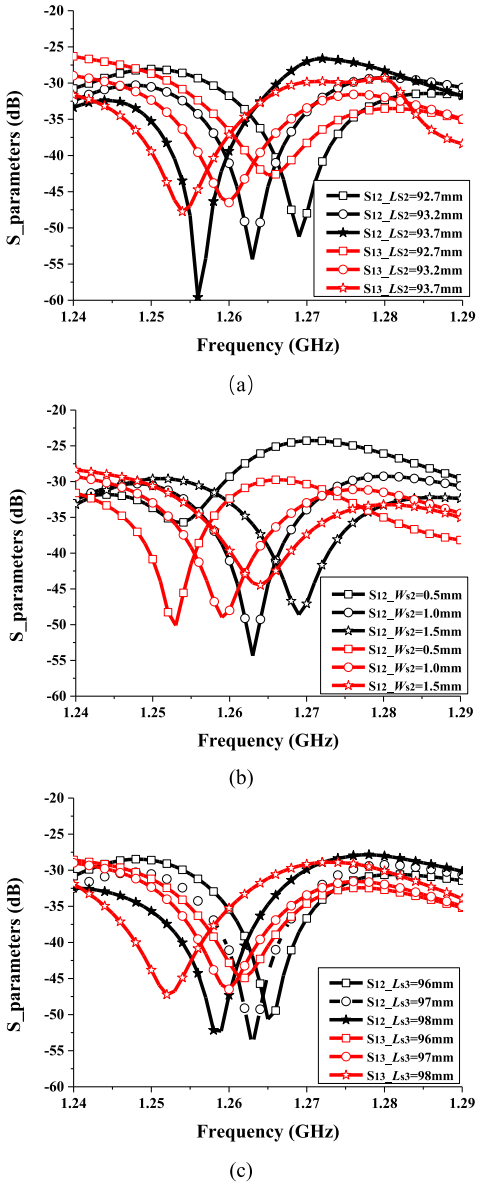

FIGURE 6. Typical scattering parameters of different size of the slot array. (a) S_{12} and S_{13} against L_{S2}. (b) S_{12} and S_{13} against W_{S2}. (c) S_{12} and S_{13} against L_{S3}.

than the above circuit analysis method is not suitable for E-plane coupled elements. Therefore, to decrease E-plane mutual coupling simultaneously, a strip array is printed on the upper surface of the substrate based on etching slot array on the ground plane.

C. THE DECOUPLING MECHANISM OF STRIP ARRAY

As shown in Fig. 1(b), five strips are printed on the same surface with patches to reduce E-plane mutual coupling. To reveal its decoupling mechanism, the vector current distribution of the antenna patch with and without the strip array at 1.264 GHz are illustrated in Fig. 8. The operating state of the antenna is that the element 1 is excited and element 2, 3, 4 is terminated with 50 Ω load. As shown in Fig. 8 (a), the coupling current on passive element

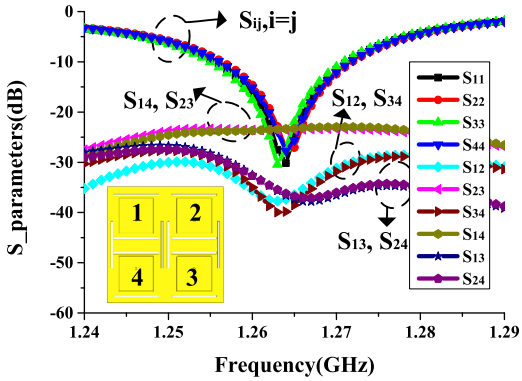

FIGURE 7. S-parameters of the antenna with slot array.

4 is co-polarized with the excitation current on neighboring element 1 which is placed along E-plane with element 4. Fig. 8(b) indicates that the proposed strip array generates induced current which is co-polarized with the excited current. Meanwhile, the phases of the induced current on the five strips are the same or opposite to the excited current. By appropriately optimizing the size and position of the strip array, the out-of-phase and the equal intensity conditions of the coupling current generated by the induced current and excited current can be achieved simultaneously, leading to a high degree of cancellation of the unwanted mutual coupling between E-plane coupled elements. In addition, the induced current of the strip array also affects the coupling current on other passive elements. Therefore, the designed strip array will further reduce the H-plane and D-plane mutual coupling. Comparing Fig. 8(a) and Fig. 8(b), the intensity of the coupling current on antenna 2, 3, 4 is significantly decreased.

Fig. 9 depicts the simulated S-parameters of the antenna with both slot array and strip array. The resonant frequency of S_{13}, S_{23} and S_{14} are at 1.26 GHz, which is 4 MHz lower than the antenna resonance frequency. This is mainly due to the slight interaction between slot array and strip array. The S_{23} and S_{14} is –54.8 dB and –49.1 dB, respectively, and about 30 dB isolation enhancement is obtained. S_{12} and S_{13} are –54.3 dB and –45.2 dB, which is also improved compared with the antenna only loading slot array. It indicates the strip array could effectively reduce E-plane mutual coupling, and further optimize the H-plane and D-plane mutual coupling. To maintain the impedance bandwidth of the antenna with DSSA, the edge length of the patches is increased by 1 mm.

The envelope correlation (ECC) provides the level of independence for each element. In MIMO antennas, ECC is used as a performance metric to characterize the system performance and efficiency. The equation to calculate ECC using S-parameters is [32]

$$\mathrm{ECC} = \rho_{ij} = \frac{\left|\sum_{n=1}^{N} S_{ni}^{*} S_{nj}\right|^2}{\left(1 - \sum_{n=1}^{N} |S_{ni}|^2\right)\left(1 - \sum_{n=1}^{N} |S_{nj}|^2\right)} \quad (2)$$

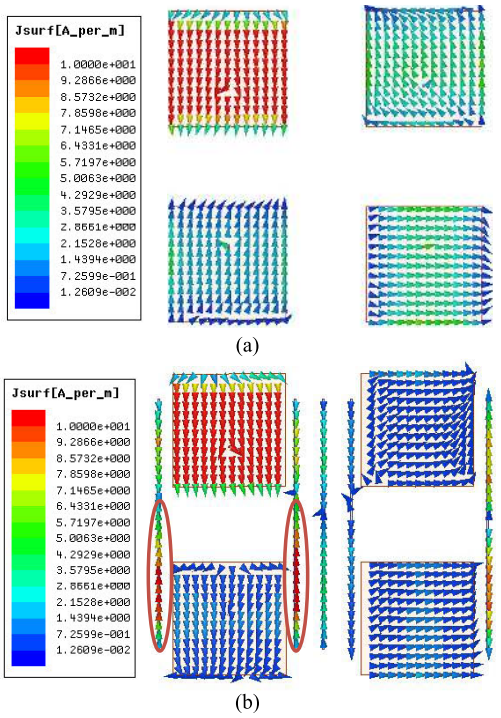

FIGURE 8. The current distribution in the plane of the antenna patch. (a) Without strip array. (b) With strip array.

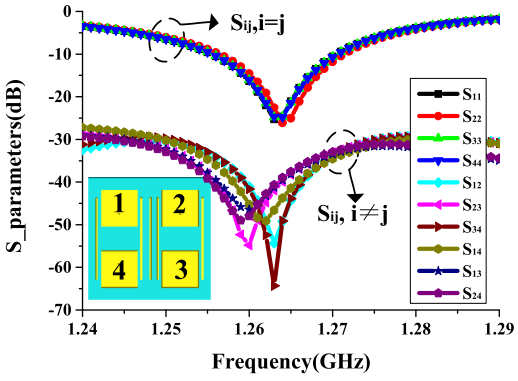

FIGURE 9. S-parameters of the antenna with both slot array and strip array.

ECC can be computed by using far-field radiation patterns with the help of equation (3) [32]

$$\mathrm{ECC} = \rho_{ij} = \frac{\left|\iint_{4\pi}\left[\vec{F}_1(\theta,\varphi)\cdot\vec{F}_2^{*}(\theta,\varphi)\,d\Omega\right]\right|^2}{\iint_{4\pi}\left|\vec{F}_1(\theta,\varphi)\right|^2 d\Omega \iint_{4\pi}\left|\vec{F}_2(\theta,\varphi)\right|^2 d\Omega} \quad (3)$$

Fig. 10 illustrates the simulated ECC for the 2 × 2 antenna with and without the proposed DSSA. Due to the symmetry of the antenna, only the representative ECC between element 1 and 2, element 1 and 3, element 1 and 4 has been given. The ECC calculated using equation (2) and (3) is found in basically agreement. The slight difference between the two results mainly comes from the antenna loss and calculation error. From the simulated results, ECC of the

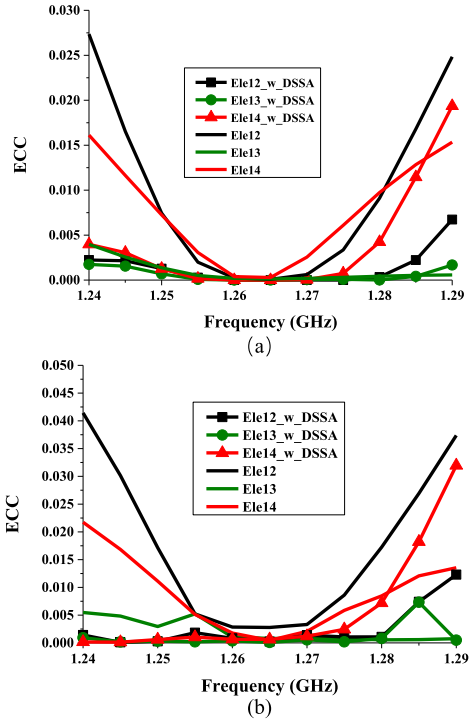

FIGURE 10. Envelope correlation of 2 × 2 antenna with and without DSSA. (a) Using equation (2). (b) Using equation (3).

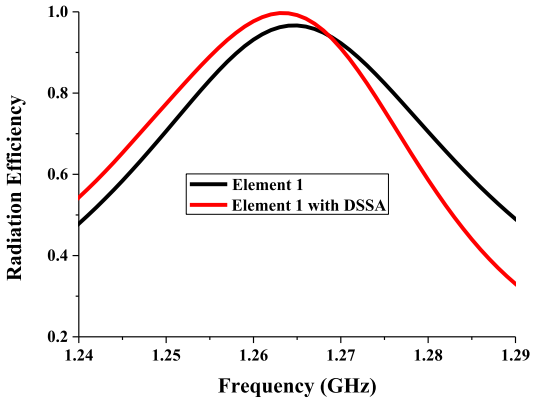

FIGURE 11. The radiation efficiency of the antenna with and without DSSA.

antenna with DSSA is smaller than that without DSSA. It is observed that the ECC of the antenna with DSSA is less than 0.005 in the working band, which indicates that the proposed DSSA can make the MIMO antenna have better diversity performance. Meanwhile, radiation efficiency is another significant performance index for antenna array. Fig. 11 displays the radiation efficiencies of element 1 with and without the proposed DSSA. The simulated results show that the radiation efficiency is improved due to the designed DSSA in the working frequency band (ignoring frequency offset) and slightly reduced in the higher frequency band. In addition, the radiation efficiency of more than 85% in the working frequency band is achieved with the DSSA.

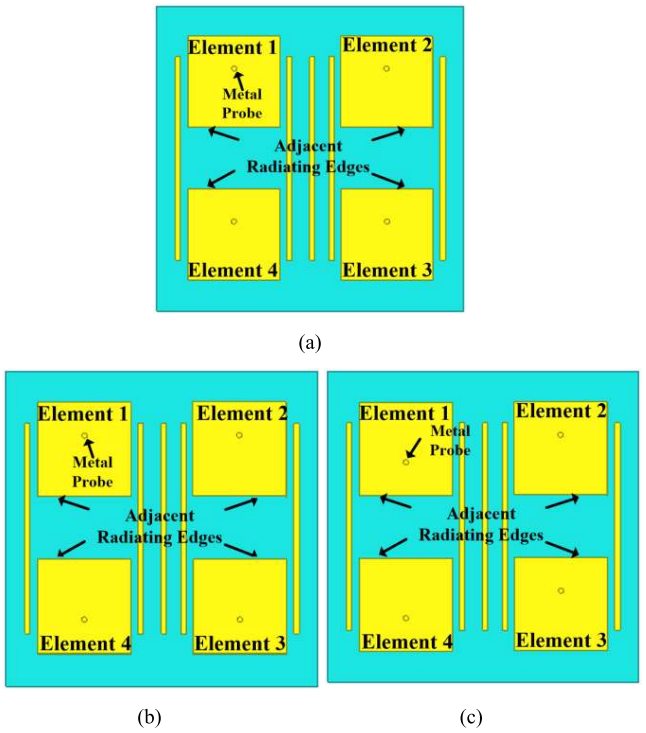

FIGURE 12. Other three types of antenna with different relative positions of feeding ports. (a) Type A. (b) Type B. (c) Type C.

D. OTHER THREE TYPES OF ANTENNA WITH DIFFERENT RELATIVE POSITIONS OF FEEDING PORTS

For an antenna array, both H-plane and E-plane array can be further classified in consideration of different relative positions of the feeding ports. In this wise, mutual coupling between array elements also varies from each other. Therefore, with this in mind, we investigated the scattering parameters of applying DSSA to other three types of antennas with different relative positions of feeding ports. We adjust the size of DSSA to reduce the mutual coupling of these three types of antenna, and the configurations shown in Fig. 12 are defined as follows (the 4 radiating edges near the center of the antenna are defined as ''adjacent radiating edges'').

1) Type A: The feeding ports of element 1, 2 are on the side away from the adjacent radiating edges and the feeding ports 3, 4 are on the side near the adjacent radiating edges.
2) Type B: The feeding ports of element 1, 2, 3, 4 are all on the side away from the adjacent radiating edges.
3) Type C: The feeding ports of element 2, 4 are on the side away from the adjacent radiating edges and the feeding ports 1, 3 are on the side near the adjacent radiating edges.

Fig. 13 shows the scattering parameters of type A, B, and C of the antenna with DSSA. The scattering parameters of the three types antenna without DSSA is almost the same as Fig. 2. It could be concluded that the reflection coefficient

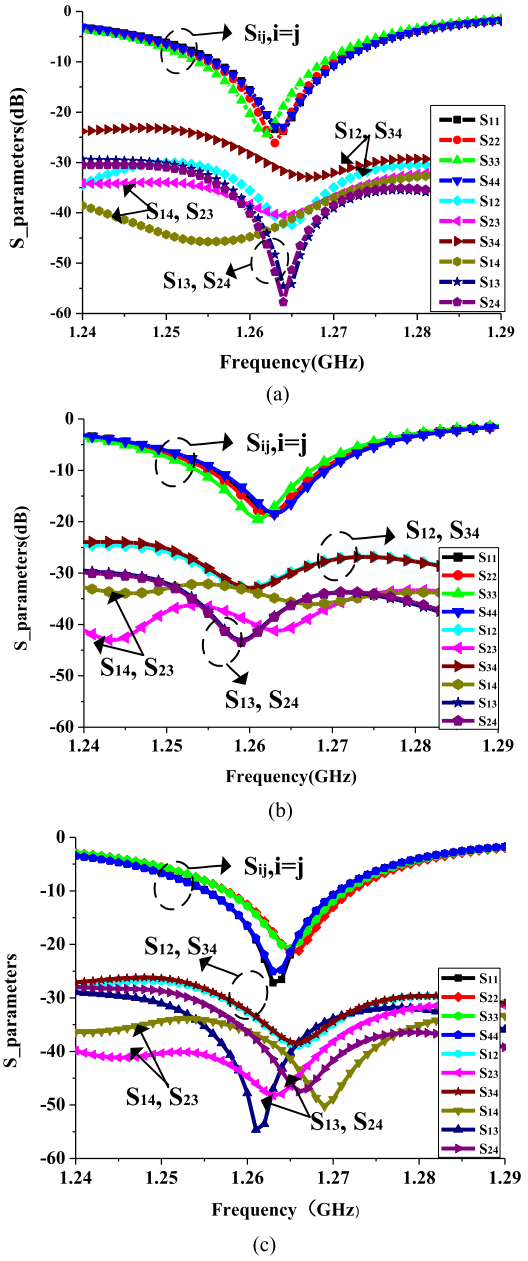

FIGURE 13. S-parameters of the other three types of antenna with DSSA. (a) Type A. (b) Type B. (c) Type C.

and bandwidth of the antenna with and without DSSA remain almost unchanged by comparing Fig. 13 and Fig. 2.

The comparison and summary of the mutual coupling coefficients are as follows.

1) Type A: The H-plane mutual coupling S_{12} and S_{34} are 42.2 dB and 32.9 dB, which improved by 26 dB and 16.7 dB, respectively. The E-plane mutual coupling S_{14} and S_{23} are 40.5 dB and 43.6 dB, and 19.5 dB and 22.5 dB isolation enhancement has been obtained. S_{13} and S_{24}, which are the D-plane mutual coupling, are 54.5 dB and 57.7 dB, and the isolation has been enhanced by about 20 dB.

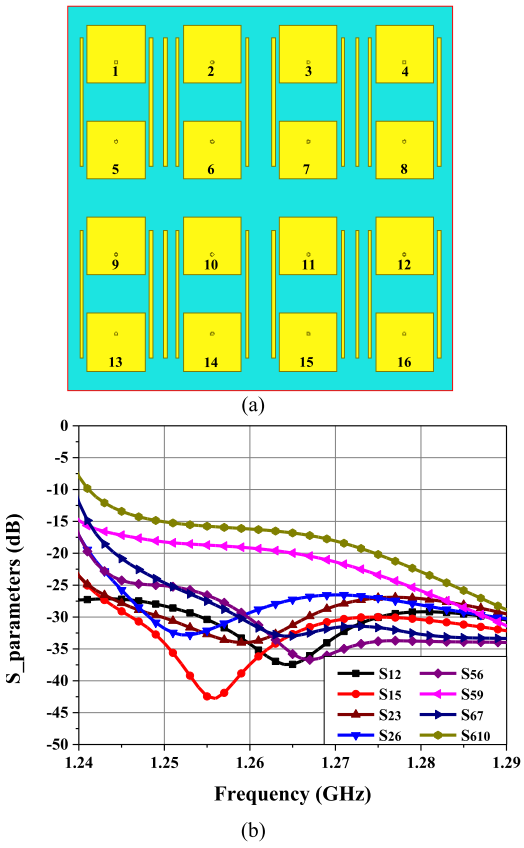

FIGURE 14. S-parameters of the 4 × 4 antenna with DSSA. (a) Top view of the geometry. (b) Typical scattering parameters.

2) Type B: The H-plane mutual coupling S_{12} and S_{34} are both 32.8 dB, which improved by 16.6 dB. The E-plane mutual coupling S_{14} and S_{23} are 41.2 dB and 35.3 dB, and 20.2 dB and 14.2 dB isolation enhancement has been obtained. S_{13} and S_{24} are both 43.2 dB, which are the D-plane mutual coupling, and the isolation has been enhanced by about 15 dB.
3) Type C: The H-plane mutual coupling S_{12} and S_{34} are both 38.9 dB, which improved by 22.7 dB. The E-plane mutual coupling S_{14} and S_{23} are 41.3 dB and 48.3 dB, 20.3 dB and 27.3 dB isolation enhancement has been obtained. S13 and S24, which are the D-plane mutual coupling, are 54.6 dB and 47.5 dB, and the isolation has been enhanced by about 20 dB.

E. THE 4 × 4 ANTENNA WITH EXTENDED DSSA

In order to verify the decoupling performance of DSSA in large-scale antenna arrays, a 4 × 4 antenna which is directly extended based on the 2 × 2 decoupling antenna is designed as shown in Fig. 14(a). The mutual coupling between typical elements is shown in Fig. 14(b). As given in the decoupling 2 × 2 antenna, the E-plane mutual coupling is about −21 dB and the H-plane mutual coupling is about −16 dB in the center frequency. Compared with the presented scattering parameters in Fig 14(b), the H-plane and part

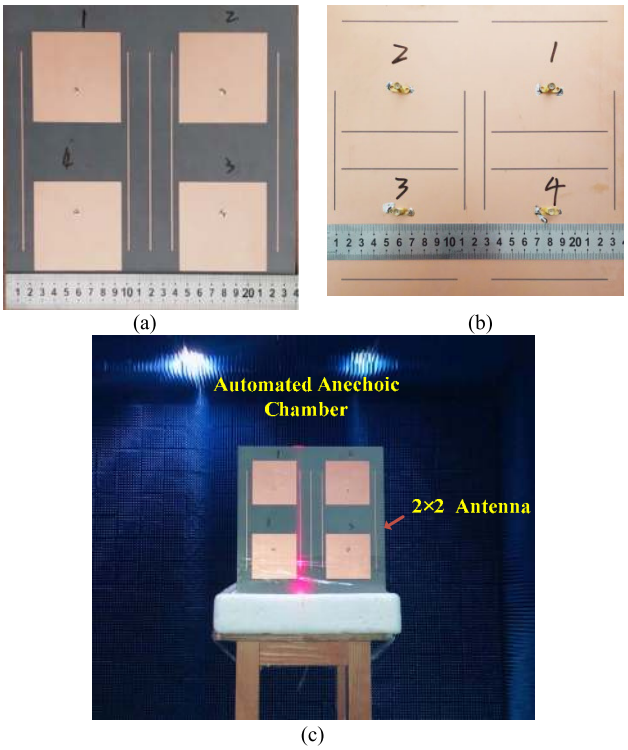

FIGURE 15. Prototype of the 2 × 2 antenna with DSSA. (a) Top view. (b) Bottom view. (c) Photograph of the measurement setup of the antenna in anechoic chamber.

of E-plane mutual coupling is decreased effectively by 10-20 dB. However, the S_{59} and S_{610} are not decreased since there is no strip array with suitable size and position between element 5 and 9, element 6 and 10. Therefore, we can conclude from the above analysis that the DSSA can effectively reduce H-plane and part of the E-plane mutual coupling in large-scale antenna such as 8 × 8 antenna and 16 × 16 antenna.

III. EXPERIMENTAL RESULTS AND DISCUSSION

A. SCATTERING PARAMETERS

To verify the performance of the proposed DSSA, a prototype is fabricated and tested as shown in Fig. 15. The S- parameters are measured using Agilent E8363B vector network analyzer. The resultant S-parameters of the antenna with and without DSSA are displayed in Fig. 16. Owing to the symmetry of the antenna, only the typical S-parameters of element 1 through element 4 are presented. The S_{12}, S_{13}, S_{14} with the DSSA are 49.4 dB, 52.3 dB, and 49.5 dB at 1.264 GHz, achieving mutual coupling reduction of 33.2 dB, 24.1 dB, and 28.5 dB compared with the antenna without DSSA, respectively. The antenna impedance bandwidth remains nearly constant. The measured results agree well with the simulated one.

B. RADIATION PATTERNS

The radiation patterns and realized gains of the fabricated 2 × 2 antenna with and without DSSA are measured in

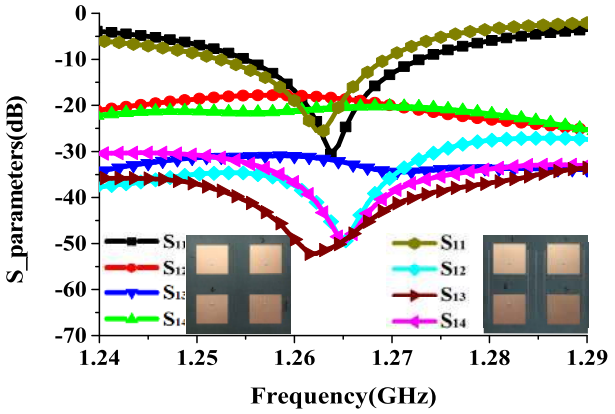

FIGURE 16. Measured S-parameters of the 2 × 2 antenna with and without slot-strip array.

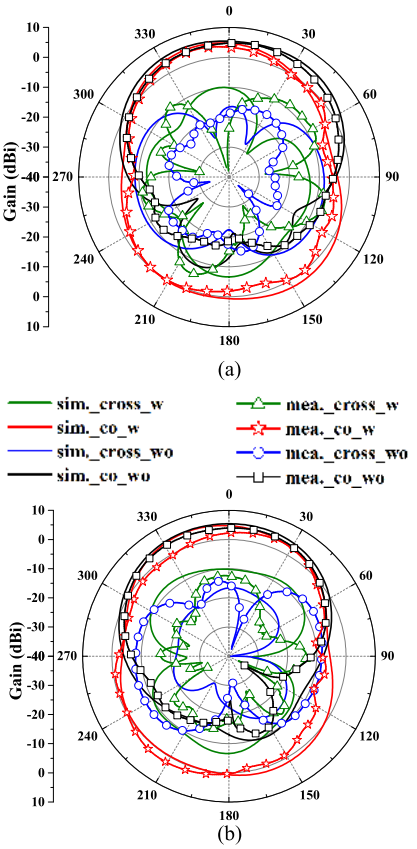

FIGURE 17. Simulated and measured radiation patterns of element 1. (a) E-plane. (b) H-plane.

automated anechoic chamber. The measured results are obtained when element 1 (see Fig. 1) is excited and other elements are terminated with a matching load. The measured and simulated radiation patterns of both E-plane and H-plane are compared at 1.264 GHz, as given in Fig. 17. In general, the measured radiation patterns are very similar to the simulated one. When the DSSA is applied, the measured gain at orientation of the antenna theta = 0° is decreased by a maximum of 0.8 dBi and 0.9 dBi (theta within ± 20°)

TABLE 2. Summaries of the mutual coupling reduction methods and their performances.

References	Method	Total size (λ_0)	Center frequency /Working band (GHz)	spacing (edge to edge) (λ_0)	Antenna type	MC reduction (center frequency)/ Lowest MC lever (dB)		
						H-plane	E-plane	D-plane
[10]	Fractal DGS	Not mentioned (two-element)	2.3 Not mentioned	0.19	Microstrip antenna		35 -52	
[12]	Polarization - conversion isolator	Not mentioned (two-element)	5.8 Not mentioned	0.17	Microstrip antenna	42.1 -57.3		
[14]	Neutralization line	0.47×0.45×0.011 (two-element)	4.05 3.1-5	0.03	Monopole	25 -40		
[16]	Neutralization line	0.32×0.72×0.006 (two-element)	3.3 2.4-4.2	0.26	Monopole	5 -34		
[19]	Metamaterial superstrate	1.6×0.9×0.16 (two-element)	3.325 3.3-3.34	0.12	Microstrip antenna		55 -70	
[23]	Decoupling surface	2.1×1.92×0.29 (2×2 antenna)	3.5 3.3-3.8	0.11,0.28	Cross-electric dipoles	25(orthogonal) -40		10(parallel) -35
[24]	Decoupling ground	2.45×2.45×0.21 (2×2 antenna)	4.9 4.6-5.2	0.38	Microstrip antenna	10 -32	8 -27	10 -40
[25]	Embedded metamaterial	4.1×3.5×0.05 (2×2 antenna)	9.54 9.12-9.96	0.64	Microstrip antenna	40 -60	7 -44.3	11 -33
[27]	Metamaterial Mushroom	0.96×0.96×0.18 (2×2 antenna)	2.42 2.396-2.45	0.44	Slot antenna	3.5(orthogonal) -52		22(parallel) -80
Present work	DSSA	1.01×1.01×0.013 (2×2 antenna)	1.264 1.256-1.272	0.2	Microstrip antenna	31.9 -49.3	22.3 -52.3	29.1 -49.5

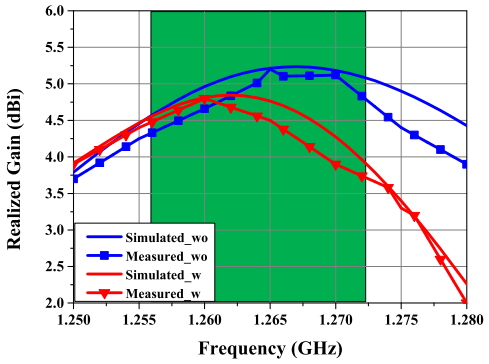

FIGURE 18. The simulated and measured realized gain versus operation band of antenna w/wo DSSA.

in E-plane and H-plane, respectively. The back-lobe levels with DSSA are larger on both E-plane and H-plane due to the inherent backward radiation of the slot-array [9], [10]. The antenna cross polarization level is nearly unchanged in E-plane and slightly degraded in H-plane compared with the antenna without DSSA. The simulation and measurement for realized gain with and without DSSA are presented in Fig. 18. The realized gain of antenna in the operating band 1.264 GHz ±8 MHz is reduced with DSSA, which is also caused by the backward radiation of the slot-array mentioned above. The measured data shows that in addition to 1.270 GHz in the working frequency band, the gain decreases within 1 dB.

IV. CONCLUSION

A low-profile decoupling DSSA for 2 × 2 microstrip antenna has been proposed in this paper, which is a composition of slot array etched on the ground plane and strip array printed on the element patches plane. By optimizing the size and position of DSSA, the mutual coupling between any two elements in four types of antenna with different relative positions of feeding ports has been decreased. The decoupling principle is via the band-stop effect of the slot array and the co-polarized induced current generated on the strip array which can cancel the coupled current. The measured results show that isolation enhancement in center frequency of 33.2 dB for H-plane, 28.5 dB for E-plane, and 24.1 dB for D-plane has been achieved with the unchanged 10 dB impedance bandwidth (1.256 GHz - 1.272 GHz). It is expected that the DSSA could be widely used in communication and radar applications.

REFERENCES

[1] I. Nadeem and D.-Y. Choi, "Study on mutual coupling reduction technique for MIMO antennas," *IEEE Access*, vol. 7, pp. 563–586, 2019.
[2] X. Chen, S. Zhang, and Q. Li, "A review of mutual coupling in MIMO systems," *IEEE Access*, vol. 6, pp. 24706–24719, 2018.
[3] P. Chen, Z. Cao, Z. Chen, and X. Wang, "Off-grid DOA estimation using sparse Bayesian learning in MIMO radar with unknown mutual coupling," *IEEE Trans. Signal Process.*, vol. 67, no. 1, pp. 208–220, Jan. 2019.
[4] J.-Y. Lee, S.-H. Kim, and J.-H. Jang, "Reduction of mutual coupling in planar multiple antenna by using 1-D EBG and SRR structures," *IEEE Trans. Antennas Propag.*, vol. 63, no. 9, pp. 4194–4198, Sep. 2015.

[5] E. Rajo-Iglesias, Ó. Quevedo-Teruel, and L. Inclan-Sanchez, "Mutual coupling reduction in patch antenna arrays by using a planar EBG structure and a multilayer dielectric substrate," *IEEE Trans. Antennas Propag.*, vol. 56, no. 6, pp. 1648–1655, Jun. 2008.
[6] H. S. Farahani, M. Veysi, M. Kamyab, and A. Tadjalli, "Mutual coupling reduction in patch antenna arrays using a UC-EBG superstrate," *IEEE Antennas Wireless Propag. Lett.*, vol. 9, pp. 57–59, 2010.
[7] K. Wei, L. Wang, Z. Xing, R. Xu, and J. Li, "S-shaped periodic defected ground structures to reduce microstrip antenna array mutual coupling," *Electron. Lett.*, vol. 52, no. 15, pp. 1288–1290, Jul. 2016.
[8] X.-J. Zou, G.-M. Wang, and Y.-W. Wang, "A novel combined structure for decoupling E/H-plane microstrip antenna array," *Int. J. RF Microw. Comput.-Aided Eng.*, vol. 28, no. 5, Jun. 2018, Art. no. e21244.
[9] A. Habashi, J. Nourinia, and C. Ghobadi, "Mutual coupling reduction between very closely spaced patch antennas using low-profile folded split-ring resonators (FSRRs)," *IEEE Antennas Wireless Propag. Lett.*, vol. 10, pp. 862–865, 2011.
[10] K. Wei, J.-Y. Li, L. Wang, Z.-J. Xing, and R. Xu, "Mutual coupling reduction by novel fractal defected ground structure bandgap filter," *IEEE Trans. Antennas Propag.*, vol. 64, no. 10, pp. 4328–4335, Oct. 2016.
[11] D. Gao, Z.-X. Cao, S.-D. Fu, X. Quan, and P. Chen, "A novel slot-array defected ground structure for decoupling microstrip antenna array," *IEEE Trans. Antennas Propag.*, early access, May 12, 2020, doi: 10.1109/TAP.2020.2992881.
[12] Y.-F. Cheng, X. Ding, W. Shao, and B.-Z. Wang, "Reduction of mutual coupling between patch antennas using a polarization-conversion isolator," *IEEE Antennas Wireless Propag. Lett.*, vol. 16, pp. 1257–1260, 2017.
[13] M. Li, B. G. Zhong, and S. W. Cheung, "Isolation enhancement for MIMO patch antennas using near-field resonators as coupling-mode transducers," *IEEE Trans. Antennas Propag.*, vol. 67, no. 2, pp. 755–764, Feb. 2019.
[14] S. Zhang and G. F. Pedersen, "Mutual coupling reduction for UWB MIMO antennas with a wideband neutralization line," *IEEE Antennas Wireless Propag. Lett.*, vol. 15, pp. 166–169, 2016.
[15] R. Liu, X. An, H. Zheng, M. Wang, Z. Gao, and E. Li, "Neutralization line decoupling tri-band multiple-input multiple-output antenna design," *IEEE Access*, vol. 8, pp. 27018–27026, 2020.
[16] C. H. See, R. A. Abd-Alhameed, Z. Z. Abidin, N. J. McEwan, and P. S. Excell, "Wideband printed MIMO/Diversity monopole antenna for WiFi/WiMAX applications," *IEEE Trans. Antennas Propag.*, vol. 60, no. 4, pp. 2028–2035, Apr. 2012.
[17] L. Zhao, L. K. Yeung, and K.-L. Wu, "A coupled resonator decoupling network for two-element compact antenna arrays in mobile terminals," *IEEE Trans. Antennas Propag.*, vol. 62, no. 5, pp. 2767–2776, May 2014.
[18] L. Zhao, F. Liu, X. Shen, G. Jing, Y.-M. Cai, and Y. Li, "A high-pass antenna interference cancellation chip for mutual coupling reduction of antennas in contiguous frequency bands," *IEEE Access*, vol. 6, pp. 38097–38105, 2018.
[19] A. Jafargholi, A. Jafargholi, and J. H. Choi, "Mutual coupling reduction in an array of patch antennas using CLL metamaterial superstrate for MIMO applications," *IEEE Trans. Antennas Propag.*, vol. 67, no. 1, pp. 179–189, Jan. 2019.
[20] F.-M. Yang, L. Peng, X. Liao, K.-S. Mo, X. Jiang, and S.-M. Li, "Coupling reduction for a wideband circularly polarized conformal array antenna with a single-negative structure," *IEEE Antennas Wireless Propag. Lett.*, vol. 18, no. 5, pp. 991–995, May 2019.
[21] M. M. Bait-Suwailam, M. S. Boybay, and O. M. Ramahi, "Electromagnetic coupling reduction in high-profile monopole antennas using single-negative magnetic metamaterials for MIMO applications," *IEEE Trans. Antennas Propag.*, vol. 58, no. 9, pp. 2894–2902, Sep. 2010.
[22] C. A. Balanis, *Antenna Theory: Analysis and Design*. Hoboken, NJ, USA: Wiley, 2005.
[23] K.-L. Wu, C. Wei, X. Mei, and Z.-Y. Zhang, "Array-antenna decoupling surface," *IEEE Trans. Antennas Propag.*, vol. 65, no. 12, pp. 6728–6738, Dec. 2017.
[24] S. Zhang, X. Chen, and G. F. Pedersen, "Mutual coupling suppression with decoupling ground for massive MIMO antenna arrays," *IEEE Trans. Veh. Technol.*, vol. 68, no. 8, pp. 7273–7282, Aug. 2019.
[25] M. Alibakhshikenari, M. Khalily, B. S. Virdee, C. H. See, R. A. Abd-Alhameed, and E. Limiti, "Mutual-coupling isolation using embedded metamaterial EM bandgap decoupling slab for densely packed array antennas," *IEEE Access*, vol. 7, pp. 51827–51840, 2019.
[26] A. Boukarkar, X. Q. Lin, Y. Jiang, L. Y. Nie, P. Mei, and Y. Q. Yu, "A miniaturized extremely close-spaced four-element dual-band MIMO antenna system with polarization and pattern diversity," *IEEE Antennas Wireless Propag. Lett.*, vol. 17, no. 1, pp. 134–137, Jan. 2018.
[27] G. Zhai, Z. N. Chen, and X. Qing, "Enhanced isolation of a closely spaced four-element MIMO antenna system using metamaterial mushroom," *IEEE Trans. Antennas Propag.*, vol. 63, no. 8, pp. 3362–3370, Aug. 2015.
[28] G. Zhai, Z. N. Chen, and X. Qing, "Mutual coupling reduction of a closely spaced four-element MIMO antenna system using discrete mushrooms," *IEEE Trans. Microw. Theory Techn.*, vol. 64, no. 10, pp. 3060–3067, Oct. 2016.
[29] A. Kumar Saurabh, P. Singh Rathore, and M. Kumar Meshram, "Compact wideband four-element MIMO antenna with high isolation," *Electron. Lett.*, vol. 56, no. 3, pp. 117–119, Feb. 2020.
[30] K. C. Gupta, R. Garg, and I. J. Bahl, *Microstrip Lines and Slotlines*. 1979.
[31] Y.-M. Yoon, H.-M. Koo, T.-Y. Kim, and B.-G. Kim, "Effect of edge reflections on the mutual coupling of a two-element linear microstrip patch antenna array positioned along the E-Plane," *IEEE Antennas Wireless Propag. Lett.*, vol. 11, pp. 783–786, 2012.
[32] S. Blanch, J. Romeu, and I. Corbella, "Exact representation of antenna system diversity performance from input parameter description," *Electron. Lett.*, vol. 39, no. 9, pp. 705–707, May 2003.

DI GAO was born in Shandong, China, in 1994. She received the B.E. degree in applied physics from Xidian University, Xi'an, China, in 2015. She is currently pursuing the Ph.D. degree with the State Key Laboratory of Millimeter Waves, Southeast University, Nanjing, China.

Her current research interests include mutual coupling reduction, phased-array antennas, and base station antennas.

ZHENXIN CAO (Member, IEEE) was born in May 1976. He received the M.S. degree from the Nanjing University of Aeronautics and Astronautics, China, in 2002, and the Ph.D. degree from the School of Information Science and Engineering, Southeast University, China, in 2005.

From 2012 to 2013, he was a Visiting Scholar with North Carolina State University. Since 2005, he has been with the State Key Laboratory of Millimeter Waves, Southeast University, where he is a Professor. His research interest includes antenna theory and application.

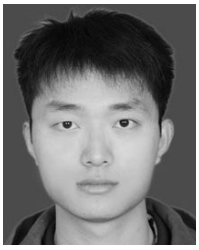

XIN QUAN was born in Henan, China, in 1993. He received the bachelor's degree in electronic information science and technology from the Nanjing University of Aeronautics and Astronautics, Nanjing, China, in 2015. He is currently pursuing the Ph.D. degree in electromagnetic field and microwave technology with Southeast University, Nanjing.

His current research interests include phased-array antennas and base station antennas.

MINQIAN SUN was born in December 1988. She received the bachelor's and master's degrees from Jiangnan University, in 2011 and 2013, respectively.

Since 2018, she has been a Lecturer with the State Key Laboratory of Disaster Prevention and Mitigation of Explosion and Impact, Army Engineering University of PLA. Her research interest includes protection engineering.

SUIDAO FU was born in Jiangsu, China, in 1990. He received the B.E. degree in electronic information science and technology from the Nanjing University of Aeronautics and Astronautics, Nanjing, China, in 2013, and the M.S. degree in electronics and communication engineering from Southeast University, Nanjing, in 2016, where he is currently pursuing the Ph.D. degree with Southeast University.

His current research interests include dual-polarized antenna, navigation antenna, and space–time adaptive anti-jamming process.

PENG CHEN (Member, IEEE) was born in Jiangsu, China, in 1989. He received the B.E. and Ph.D. degrees from the School of Information Science and Engineering, Southeast University, China, in 2011 and 2017, respectively. From March 2015 to April 2016, he was a Visiting Scholar with Electrical Engineering Department, Columbia University, New York, NY, USA.

He is currently an Associate Professor with the State Key Laboratory of Millimeter Waves, Southeast University. His research interests include radar signal processing and millimeter wave communication.